Article

Cite This: Biomacromolecules 2018, 19, 2089−2097

pubs.acs.org/Biomac

Salt- and pH-Triggered Helix−Coil Transition of Ionic Polypeptides under Physiology Conditions

Jingsong Yuan,[†] Yi Zhang,[†] Yue Sun,[†] Zhicheng Cai,[‡] Lijiang Yang,*[,‡] and Hua Lu*[,†]

[†]Center for Soft Matter Science and Engineering, Key Laboratory of Polymer Chemistry and Physics of Ministry of Education and [‡]Institute of Theoretical and Computational Chemistry, Biodynamic Optical Imaging Center, Beijing National Laboratory for Molecular Sciences, College of Chemistry and Molecular Engineering, Peking University, Beijing 100871, People's Republic of China

Supporting Information

ABSTRACT: Controlling the helix−coil transition of polypeptides under physiological conditions is an attractive way toward smart functional materials. Here, we report the synthesis of a series of tertiary amine-functionalized ethylene glycol (EG_x)-linked polypeptide electrolytes with their secondary structures tunable under physiological conditions. The resultant polymers, denoted as P(EG_xDMA-Glu) (x = 1, 2, and 3), show excellent aqueous solubility (>20 mg/mL) regardless of their charge states. Unlike poly-L-lysine that can form a helix only at pH above 10, P(EG_xDMA-Glu) undergo a pH-dependent helix−coil switch with their transition points within the physiological range (pH ∼5.3−6.5). Meanwhile, P(EG_xDMA-Glu) exhibit an unusual salt-induced helical conformation presumably owing to the unique properties of EG_x linkers. Together, the current work highlights the importance of fine-tuning the linker chemistry in achieving conformation-switchable polypeptides and represents a facile approach toward stimuli-responsive biopolymers for advanced biological applications.

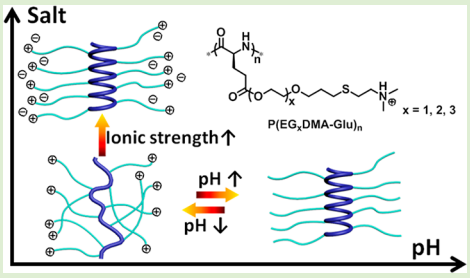

INTRODUCTION

The α-helical conformation of polypeptides/proteins is a pivotal structural motif that governs a wide range of biological functions such as enhancing protein−ligand binding, regulating protein−protein interaction, and enabling membrane activity of antimicrobial peptides.[1−7] Often, the onset of these biological functions is regulated by the coil-to-helix transition of the peptides.[8−10] One vivid example is perhaps the pH-dependent transmembrane activity of pH low insertion peptides (pHLIPs), a family of peptides that undergo a sharp coil-to-helix transition when the pH is lowered from 7.4 to 6.0.[11−13] Inspired by this, it is intriguing to mimic such natural behaviors in artificial systems under physiological conditions.[14−16] For synthetic polypeptides made by the ring-opening polymerization (ROP) of α-amino acid *N*-carboxyanhydrides (NCAs),[17−24] however, the transitions often occur under conditions far from those of the physiological environment. For example, poly-L-lysine (PLL) can form a helix only at a pH above 10 when its side-chain ammoniums are deprotonated to neutral amines. This, unfortunately, also leads to significantly decreased aqueous solubility. As such, charged PLL always adopts the less interesting coil conformation under physiological conditions. In addition, the helicity of PLL is vulnerable to various environmental stresses including high ionic strength and elevated temperature.[25] To address this dilemma, Lu and Cheng have previously constructed ultrastable helices by using ionic polypeptides with elongated hydrophobic linkers.[26] They have concluded that a hydrophobic linker separating the charge and the peptide backbone with a charge-to-backbone distance (CBD) of minimum 11 σ bonds is crucial to creating a stable helix resistant to various environmental stresses. However, these helices lack the sometimes desired dynamics such as the coil-to-helix transition. Moreover, the greasy hydrophobic linker can produce considerable synthetic hurdles and lead to problems such as toxicity and poor water solubility.

To manipulate the helix−coil transition in neutral polypeptides, Deming and Li exploited the redox responsiveness of the thioether group in L-cysteine-derived polypeptides.[27,28] Our group previously showed that a photoresponsive helix−coil transition was realizable by introducing an azobenzene group in the side chain.[29] Metallic coordination was also explored to achieve helix−coil transition.[30] For ionic polypeptides, Schlaad et al. took advantage of the Columbic interaction in glycosylated copoly(L-glutamate)s.[31,32] Bonduelle et al. investigated the charge repulsion among side chain imidazole groups.[33] Cheng and co-workers showed that such a transition was achievable by imparting both hydrogen donor and acceptor in the side chain of ionic homopolypeptides.[34] Here, we hypothesize that ionic homopolypeptides with fine-tuned amphiphilicity and linker length can realize switchable helix−coil transition under physiological conditions. For this purpose, we reason that oligo(ethylene glycol) (EG_x) is an ideal linker candidate. Although poly(ethylene glycol) (PEG) is widely considered as a hydrophilic polymer, numerous studies have shown that the hydration status of PEG varied under different

Special Issue: Biomacromolecules Asian Special Issue

Received: February 6, 2018
Revised: March 22, 2018
Published: March 26, 2018

DOI: 10.1021/acs.biomac.8b00204
Biomacromolecules 2018, 19, 2089−2097

Scheme 1. Synthesis of the EG_xene-GluNCA Monomers and the Ionic P(EG_xDMA-Glu) Polypeptides

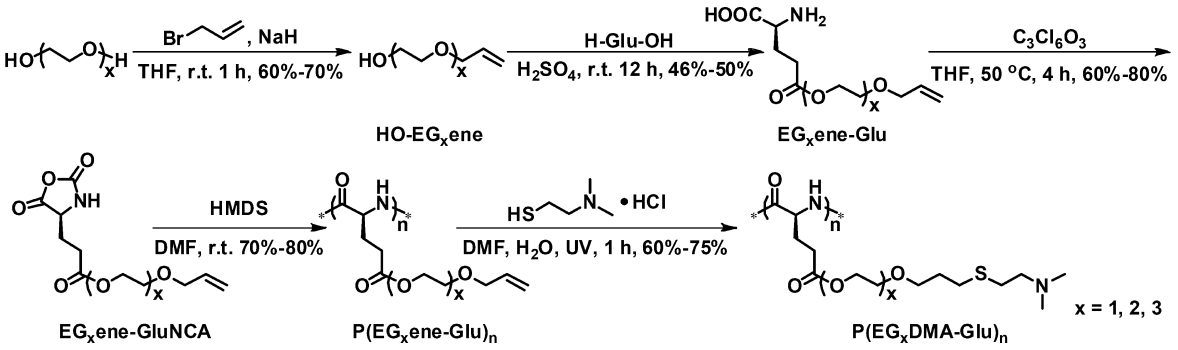

physicochemical environments such as ionic strength and temperature.[35−38] As such, we designed a series of ionic poly(L-glutamate) derivatives bearing EG_x linkers of various lengths (x = 1−3), which correspondingly give rise to CBDs ranging from 14 to 30 sigma bonds, respectively (Scheme 1). We show that the secondary structure of the polypeptides can be switched by pH and salt as demonstrated by circular dichroism (CD) spectroscopy, 2D nuclear overhauser effect spectroscopy (NOESY), and molecular dynamics (MD).

MATERIALS AND METHODS

Materials. All chemicals were purchased from commercial sources and used as received unless otherwise specified. Ultrapure water (15.0 MΩ, Milli-Q) was used in all experiments. HMDS and anhydrous *N*,*N*-dimethylformamide (DMF) were purchased from Sigma-Aldrich (St. Louis, MO, U.S.A.). Anhydrous dichloromethane (DCM), hexane, and tetrahydrofuran (THF) were obtained by passing HPLC-grade solvents through columns packed with neutral alumina or activated 4 Å molecular sieves. 2,2-Dimethoxy-2-phenylacetophenone (DMPA) was purchased from Aladdin Reagent Co. Ltd. (Shanghai, China). Poly-L-lysine was prepared by the ring-opening polymerization of ε-carboxybenzyl L-lysine NCA (Z-LysNCA) and subsequently deprotected following a previously reported procedure.[39]

Characterizations. NMR spectra were recorded on a 400 MHz Bruker ARX400 or a 500 MHz AVANCE III FT-NMR spectrometer. Fourier transform infrared spectroscopy (FT-IR) was recorded using a Bruker Tensor FT-IR spectrometer (Bruker, Bremen, Germany) in the range of 400−4000 cm^{-1} at a resolution of 2 cm^{-1} and 32 scans. Tandem gel permeation chromatography (GPC) experiments were performed on a system equipped with an isocratic pump (Model 1100, Agilent Technology, Santa Clara, CA), a DAWN HELEOS 9-angle laser light scattering detector (also known as multiangle laser light scattering (MALLS) detector, Wyatt Technology, Santa Barbara, CA), and an Optilab rEX refractive index detector (Wyatt Technology, Santa Barbara, CA). The detection wavelength of MALLS was set at 658 nm. The temperature of both the refractive index and the MALLS detectors was 25 °C. Separations were performed using serially connected size exclusion columns (500, 10^3,10^4, and 10^5 Å Phenogel columns, 5 μm, 7.8 × 300 mm, Phenomenex, Torrance, CA) at 50 °C using DMF containing 0.1 M LiBr as the mobile phase. The molecular weights (MWs) of all polymers were determined based on the d*n*/d*c* values of all samples calculated offline by using the internal calibration system processed by the ASTRA V software version 5.1.7.3 provided by Wyatt Technology. Circular dichroism (CD) spectroscopy was carried out on a Bio−Logic MOS 450 CD spectrometer. The polymer solution was placed in a quartz cell with a light path of 1.0 cm. The mean residue molar ellipticity was calculated by the following formula: ellipticity ($[\theta]$ in deg cm^2 $dmol^{-1}$) = (millidegrees × mean residue weight)/(path length in millimeters × concentration of polypeptide in mg/mL). The α-helix contents of polypeptides were calculated using the following equation: % α-helix = 100% × $(-[\theta_{222}] + 3000)/39000$.

Experimental Section. *General Procedure for the Preparation of HO-EG_xene.* Taking HO-EG_3ene (2-(2-(2-(allyloxy)ethoxy)-ethoxy)ethanol) as an example, to an ice-bath solution of triethylene glycol (45.0 g, 300 mmol, 3.0 equiv) in THF (100 mL) was added sodium hydride (3.8 g, 160 mmol, 1.6 equiv) in one portion. The reaction was kept stirring at room temperature for 15 min, after which 3-bromopropene (12 g, 100 mmol, 1.0 equiv) was added to the solution. After stirring for another 1 h, the solvent was removed by evaporation. The residue was dissolved in DCM (200 mL), and the solid was removed by filtration. The organic phase was washed with saturated NaCl and water (100 mL). The water phase was extracted with DCM for another two times (200 mL). The organic phase was combined and dried with Na_2SO_4. After evaporating the solvent, the crude product was purified by chromatography (petroleum ether (PE): ethyl acetate (EA) = 7:3−1:1) to afford the pure product as a colorless oil (11.4 g, yield 60%). ^{1}H NMR (400 MHz, $CDCl_3$) δ 5.93 (ddt, *J* = 16.1, 10.9, 5.7 Hz, 1H), 5.28 (dd, *J* = 17.2, 1.5 Hz, 1H), 5.19 (d, *J* = 10.4 Hz, 1H), 4.03 (d, *J* = 5.7 Hz, 2H), 3.80−3.53 (m, 12H), 2.62 (s, 1H). ^{13}C NMR (126 MHz, $CDCl_3$) δ 134.79, 117.35, 72.65, 72.39, 70.77, 70.73, 70.48, 69.51, 61.88. ESI-MS: calculated *m*/*z* 190.1; found *m*/*z* 213.2 $[M + Na]^+$.

HO-EG_2ene (2-(2-(Allyloxy)ethoxy)ethanol). ^{1}H NMR (400 MHz, $CDCl_3$) δ 5.91 (ddt, *J* = 16.1, 10.4, 5.8 Hz, 1H), 5.29 (dd, *J* = 17.2, 1.5 Hz, 1H), 5.20 (dd, *J* = 10.4, 1.0 Hz, 1H), 4.04 (d, *J* = 5.7 Hz, 2H), 3.70 (m, 8H), 2.51 (s, 1H). ^{13}C NMR (126 MHz, $CDCl_3$) δ 134.65, 117.49, 72.64, 72.40, 70.61, 69.61, 61.94. ESI-MS: calculated *m*/*z* 146.1; found *m*/*z* 169.2 $[M + Na]^+$.

HO-EG_1ene (2-(Allyloxy)ethanol). This compound was purchased from Aladdin Reagent Co. Ltd. (Shanghai, China) and used directly.

General Procedure for the Preparation of EG_xene-Glu. Taking EG_3ene-Glu (γ-(2-(2-(2-allyloxyethoxy)ethoxy)ethoxy)-L-glutamate) as an example, to a solution of L-glutamate (3.0 g, 34 mmol, 1.0 equiv) suspended in 2-(2-(2-(allyloxy)ethoxy)ethoxy)ethanol (11.4 g, 60 mmol, 2.94 equiv) at 0 °C was added sulfuric acid (1.8 g, 33.7 mmol, 1.65 equiv) dropwise over 10 min. After stirring at room temperature overnight, the viscous solution was poured slowly into mixed triethylamine (6.81 g, 67.4 mmol, 3.3 equiv) and isopropanol (250 mL) to yield a white precipitate that was collected by high speed centrifugation and dried under vacuum. EG_3ene-Glu was purified by recrystallization in methanol/diethyl ether (*v*/*v*: 50/200) and completely dried (6.5 g, yield 46%). The amino acid should be used within a few days; otherwise, it should be kept under desiccators to avoid moisture. ^{1}H NMR (400 MHz, D_2O) δ 5.85 (ddt, *J* = 16.5, 10.6, 6.0 Hz, 1H), 5.24 (dd, *J* = 17.2, 1.5 Hz, 1H), 5.16 (d, *J* = 10.4 Hz, 1H), 4.18 (t, *J* = 6.0 Hz, 2H), 3.97 (d, *J* = 6.0 Hz, 2H), 3.71−3.54 (m, 11H), 2.50 (t, *J* = 7.7, 2H), 2.06 (m, 2H). ^{13}C NMR (126 MHz, D_2O) δ 174.51, 173.77, 133.67, 118.44, 71.74, 69.64, 69.60, 69.51, 68.70, 68.42, 64.08, 53.90, 29.79, 25.40. ESI-MS: calculated *m*/*z* 319.2; found *m*/*z* 320.2 $[M + H]^+$.

EG_2ene-Glu (γ-(2-(2-Allyloxyethoxy)ethoxy)-L-glutamate). ^{1}H NMR (400 MHz, D_2O) δ 5.84 (ddt, *J* = 16.5, 10.7, 5.7 Hz, 1H), 5.23 (dd, *J* = 17.2, 1.5 Hz, 1H), 5.16 (dd, *J* = 10.4, 1.0 Hz, 1H), 4.19 (t, 2H), 3.96 (d, *J* = 5.9 Hz, 2H), 3.68 (m, 3H), 3.60 (m, 4H), 2.50 (t, *J* = 7.7, 2H), 2.07 (m, 2H). ^{13}C NMR (126 MHz, D_2O) δ 174.53, 173.79, 133.68, 118.38, 71.72, 69.61, 68.60, 68.38, 64.05, 53.90, 29.78, 25.40. ESI-MS: calculated *m*/*z* 275.1; found *m*/*z* 276.1 $[M + H]^+$.

DOI: 10.1021/acs.biomac.8b00204
Biomacromolecules 2018, 19, 2089−2097

EG_1ene-Glu (γ-(2-Allyloxyethoxy)-L-glutamate). ^{1}H NMR (400 MHz, D_2O) δ 5.84 (ddt, J = 16.4, 10.5, 6.0 Hz, 1H), 5.23 (dd, J = 17.2, 1.5 Hz, 1H), 5.17 (dd, J = 10.4, 1.0 Hz, 1H), 4.20 (t, 2H), 3.98 (d, J = 5.9 Hz, 2H), 3.67 (m, 3H), 2.50 (t, J = 7.9, 2H), 1.98 (m, 2H). ^{13}C NMR (126 MHz, D_2O) δ 174.53, 173.80, 133.48, 118.58, 71.71, 67.54, 64.10, 53.89, 29.77, 25.41. ESI-MS: calculated m/z 231.1; found m/z 232.2 $[M + H]^+$.

General Procedure for the Preparation of EG_xene-GluNCA. Taking EG_3ene-GluNCA (γ-(2-(2-(2-allyloxyethoxy)ethoxy)ethoxy)-L-glutamate *N*-carboxyanhydride) as an example, to a mixture of EG_3ene-Glu (1.0 g, 3.1 mmol, 1.0 equiv) and triphosgene (344 mg, 1.16 mmol, 0.37 equiv) under nitrogen were added anhydrous THF (30 mL) and α-pinene (641 mg, 4.7 mmol, 1.5 equiv). The solution was then heated to 50 °C for 3−5 h after which the solvent was removed under vacuum. The yellow oil was dissolved in a minimal amount of DCM and purified by chromatography with the room humidity under 50%. The NCA was eluted with mixed PE and EA (0.87 g, yield 80%). The pure NCA fractions were immediately combined and dried under vacuum. The pure NCA was transferred into the glovebox and stored in a refrigerator under −20 °C. ^{1}H NMR (400 MHz, $CDCl_3$) δ 7.32 (s, 1H), 5.90 (ddt, J = 16.1, 10.4, 5.8 Hz, 1H), 5.28 (dd, J = 17.2, 1.5 Hz, 1H), 5.19 (d, J = 10.4 Hz, 1H), 4.47 (t, J = 5.8 Hz, 1H), 4.33 (m, 2H), 4.01 (t, J = 5.8 Hz, 2H), 3.77−3.49 (m, 10H), 2.64−2.42 (m, 2H), 2.32−2.42 (m, 1H), 2.16−2.04 (m, 1H). ^{13}C NMR (126 MHz, $CDCl_3$) δ 171.93, 170.41, 151.95, 134.55, 117.71, 72.32, 70.64, 70.56, 70.36, 69.44, 68.81, 63.64, 57.32, 30.51, 27.17. FT-IR (cm^{-1}): 2934, 2873, 2678, 1738, 1609, 1584, 1511, 1412, 1325, 1113, 996, 923. ESI-MS: calculated m/z 345.1; found m/z 368.2 $[M + Na]^+$.

EG_2ene-GluNCA (γ-(2-(2-Allyloxyethoxy)ethoxy)-L-glutamate N-carboxyanhydride). ^{1}H NMR (400 MHz, $CDCl_3$) δ 7.09 (s, 1H), δ 5.90 (ddt, J = 16.5, 10.7, 5.7 Hz, 1H), 5.28 (dd, J = 17.2, 1.5 Hz, 1H), 5.20 (dd, J = 10.4, 1.0 Hz, 1H), 4.43−4.20 (m, 3H), 4.01 (t, J = 5.7 Hz, 2H), 3.82−3.50 (m, 6H), 2.63−2.32 (m, 3H), 2.13 (m, 1H). ^{13}C NMR (101 MHz, $CDCl_3$) δ 171.85, 170.07, 151.73, 134.40, 117.56, 72.18, 70.22, 69.31, 68.71, 63.56, 57.34, 30.55, 27.03. ESI-MS: calculated m/z 301.1; found m/z 324.2 $[M + Na]^+$.

EG_1ene-GluNCA (γ-(2-Allyloxyethoxy)-L-glutamate N-carboxyanhydride). ^{1}H NMR (400 MHz, $CDCl_3$) δ 6.84 (s, 1H), 5.92 (ddt, J = 16.2, 10.4, 5.8 Hz, 1H), 5.30 (dd, J = 17.2, 1.5 Hz, 1H), 5.24 (dd, J = 10.4, 1.0 Hz, 1H), 4.43−4.34 (m, 2H), 4.22 (m, 1H), 4.10 (m, 2H), 3.69 (m, 2H), 2.58 (t, J = 5.8 Hz, 2H), 2.38 (m, 1H), 2.12 (m, 1H). ^{13}C NMR (101 MHz, $CDCl_3$) δ 172.05, 169.90, 151.45, 133.97, 118.47, 72.27, 67.41, 64.10, 57.67, 31.09, 27.46. ESI-MS: calculated m/z 257.1; found m/z 280.1 $[M + Na]^+$.

General Procedure for the Polymerization of EG_xene-GluNCA. Taking EG_3ene-GluNCA as an example, in a glovebox, EG_3ene-GluNCA (200 mg, 0.580 mmol, 50 equiv) dissolved in anhydrous DMF (2 mL) was added to a HMDS stock solution in DMF (23.2 μL × 0.5 M, 1.0 equiv) and stirred for 15 h at room temperature. Upon complete consumption of the monomer as monitored by FT-IR spectroscopy, an aliquot of the reaction mixture was diluted to 5 mg/mL in DMF containing 0.1 M LiBr and injected for GPC analysis. To obtain the purified P(EG_3ene-Glu), the reaction solution was poured into diethyl ether (80 mL), and the precipitate was collected by centrifugation, washed extensively with diethyl ether (40 mL × 2), and dried under vacuum (yields ∼70%). The polymer could be stored in a −20 °C freezer for up to 2 months. ^{1}H NMR (400 MHz, $CDCl_3$) δ 5.93 (m, 1H), 5.31−5.14 (m, 2H), 4.23 (br, 3H), 4.01 (br, 2H), 3.72−3.56 (br, 10H), 2.75−1.95 (br, 4H).

P(EG_2ene-Glu). ^{1}H NMR (400 MHz, d_6-DMSO) δ 8.09 (br, 1H), 5.86 (m, 1H), 5.27−5.08 (m, 2H), 4.24 (br, 1H), 4.12 (br, 2H), 3.92 (br, 2H), 3.54 (m, 6H), 2.35 (br, 2H), 2.10−1.70 (br, 2H).

P(EG_1ene-Glu). ^{1}H NMR (400 MHz, d_6-DMSO) δ 8.20 (br, 1H), 5.84 (m, 1H), 5.27−5.09 (m, 2H), 4.30−4.15 (br, 3H), 3.94 (br, 2H), 3.54 (br, 2H), 2.37 (br, 2H), 2.10−1.70 (br, 2H).

General Procedure for the Synthesis of P(EG_xDMA-Glu)$_{50}$. Taking P(EG_3DMA-Glu)$_{50}$ as an example, P(EG_3ene-Glu)$_{50}$ (20.0 mg, 0.0653 mmol "ene", 1.0 equiv), *N*,*N*-dimethyl mercaptoehtylamine hydrochloride (37.0 mg, 0.0.261 mmol, 4.0 equiv), and dimethoxy phenyl acetophenone (DMPA, 1.8 mg, 0.007 mmol, 0.11 equiv) were dissolved in a DMF/water mixture (400/40 μL) in a 5 mL vial. The vial was capped, and the mixture was irradiated with a 365 nm UV lamp (1.0 W/cm^2) for 0.5 h. The reaction could be continued for another 0.5 h irradiation with the addition of another 1.8 mg of DMPA if necessary. The product was purified using a PD-10 column and lyophilized to afford the product as a white gel-like solid (20 mg, yield 75%). ^{1}H NMR (400 MHz, D_2O) δ 4.31 (br, 1H), 4.22 (br, 2H), 3.73 (br, 2H), 3.54−3.68 (m, 10H), 3.33 (t, J = 5.7 Hz, 2H), 2.90−2.84 (m, 8H), 2.62 (t, J = 5.7 Hz, 2H), 2.49 (br, 2H), 2.17−1.92 (m, 2H), 1.83 (q, J = 5.7 Hz, 2H).

P(EG_2DMA-Glu)$_{50}$. ^{1}H NMR (400 MHz, D_2O) δ 4.31 (br, 1H), 4.20 (br, 2H), 3.70 (br, 2H), 3.50−3.65 (m, 6H), 3.31 (t, J = 5.7 Hz, 2H), 2.84 (m, 8H), 2.60 (t, J = 5.7 Hz, 2H), 2.46 (br, 2H), 2.20−1.90 (m, 2H), 1.81 (q, J = 5.7 Hz, 2H).

P(EG_1DMA-Glu)$_{50}$. ^{1}H NMR (500 MHz, D_2O) δ 4.33 (br, 1H), 4.26 (br, 2H), 3.68 (br, 2H), 3.58 (t, J = 7.2 Hz, 2H), 3.29 (t, J = 5.7 Hz, 2H), 2.87−2.80 (m, 8H), 2.61 (t, J = 5.7 Hz, 2H), 2.48 (br, 2H), 2.15−1.90 (m, 2H), 1.82 (q, J = 5.7 Hz, 2H).

CD Spectroscopy. Polypeptides were dissolved in DI water at a concentration of 0.05 mg/mL. The pH value of the solution was adjusted by adding a specific volume of concentrated HCl or NaOH, and the solution pH was measured by a pH meter (Oakton Instruments, Vernon Hills, IL, USA). After the pH was adjusted to the desired value, the polypeptide solution was transferred to a quartz cuvette (path length = 1 or 10 mm) for CD tests at 25 °C. For the temperature-dependent CD measurement, the temperature of the sample chamber where the quartz cuvette was placed was controlled by a water bath with a programmed heating ramp. The samples were equilibrated at each temperature for at least 10 min before measurement.

pH Titration and Apparent pK_a Measurement. The pH titration experiments were conducted by following a previously reported procedure.[40] Briefly, P(EG_xDMA-Glu)$_{50}$ or PLL_{50} (5 mg) was dissolved in HCl (0.1 M × 5 mL) to adjust the initial pH of the polymer solution below 4.0. Then, NaCl (8.8 mg) was added to the solution to adjust the salt concentration to ∼150 mM. The pH titration was carried out by adding small aliquots (5 μL increment) of NaOH solution (0.1 M for P(EG_xDMA-Glu)$_{50}$) or 1 M for PLL_{50}) at 25 °C. The solution pH, measured by a pH meter, was plotted as a function of the total added volume of NaOH.

NOESY Experiments. P(EG_xDMA-Glu)$_{50}$ for NOESY were dissolved in D_2O at 10 mg/mL. 2D NOESY experiments were performed on a 500 MHz AVANCE III FT-NMR spectrometer with a Cyro-probe. The pulse sequence was noesygpph19 with an acquisition time of 107 and 26.7 ms. The $\pi/2$ pulse width was 8.85 μs. The recycle delay was 2.0 s, and τ_m was 100 ms.

Simulation of P(EG_3DMA-Glu)$_{20}$. We used the Amber 14 Molecular Dynamics Package to perform the all-atom simulation of the polypeptide. To build the initial polypeptide configuration, we used Gaussview to generate side-chain coordinates, and Gaussian 09 to optimize the side-chain configuration at a HF/6-31G* level of theory. Then, the side-chain was grafted to a helical backbone template by Amber14. The polypeptide was modeled with the Amber force field augmented with some nonbonded interactions computed using the RESP ESP charge Derive Server (R.E.D.Server, http://upjv.q4md-forcefieldtools.org/REDServer-Development/). The backbone was simulated using force field parm10.dat, and the side-chain was simulated using force field gaff.dat. Partial charges were assigned from quantum mechanical predictions using Firefly_7.1.G on the R.E.D.Server. The polypeptide has a net charge of +21e due to the positively charged terminal group on each side-chain and on the *N*-terminal of the backbone. The net charge was neutralized by adding Na^+ and Cl^- ions. The whole system was placed in a box with periodic boundary conditions and solvated by TIP3P water molecules at 298 K and 1 bar.

Cytotoxicity Experiments. In a 5% CO_2-containing humidified atmosphere, HeLa cells were grown in Dulbecco's modified Eagle medium (DMEM, Corning, Manassas, US) supplemented with 10% fetal bovine serum (FBS), and 4T1 cells were maintained in RPMI

DOI: 10.1021/acs.biomac.8b00204
Biomacromolecules 2018, 19, 2089−2097

1640 (Corning, US) supplemented with 10% FBS at 37 °C. Cells were seeded at a density of 5000 cells/well for 24 h in a 96-well plate prior to the experiment to allow complete cell attachment to the plate. The cells were incubated with P(EG_xDMA-Glu)$_{50}$ at appropriate concentrations for 24 h with fresh medium added (n = 3). The cell viabilities relative to the untreated group (100%) were determined by 3-(4,5-dimethylthiazol-2-yl)-2,5-diphenyltetrazolium bromide (MTT) assay following the manufacturer's procedure.

Membrane Activity Experiments. The LUV was received as a kind gift from Dr. Yuting Sun and used directly, which was prepared following a general procedure described below: The thin lipid film was prepared by evaporating a lipid mixture (25 mg, DOPC:cholesterol:DSPE-PEG2000 = 50:50:5) in 1 mL mixed MeOH/$CHCl_3$ (volume ratio = 1:1) on a rotary evaporator at room temperature. Thereafter, the thin lipid film was further dried in vacuo overnight. The resulting film was dissolved in 1.0 mL buffer containing 50 mM 5(6)-carboxyfluorescein (CF), 10 mM Tris, and 10 mM NaCl (pH 7.4) for more than 30 min and then subjected to several times (usually more than 5) of freeze−thaw cycles. The LUV was then extruded through a polycarbonate membrane with a pore size of 200 nm for more than 20 times. Extravesicular components were removed by passing a Sephadex G-50 filled column with 10 mM Tris, 107 mM NaCl, pH 7.4 buffer as eluent.

The membrane activity experiments were conducted by following a previously reported procedure.[41] LUV stock solution (10 μL) was diluted 10000-fold with a buffer containing 10 mM Tris and 107 mM NaCl (pH 7.4) with a final lipid concentration of 0.5 μM. The CF efflux was monitored at λ_{em} 517 nm after mixing the diluted LUV solution (10 μL), Tris buffer (80 μL with 10 mM Tris, 107 mM NaCl, pH 7.4) and polypeptide solutions at different concentrations (10 μL, 10 mM Tris, 107 mM NaCl, pH 7.4) for 2 min. The 100% CF efflux was determined by using 1.0% aqueous triton X-100 (10 μL, 10 mM Tris, 107 mM NaCl, pH 7.4) instead of the polypeptide solution. Effective concentration for polypeptide EC_{50} and Hill coefficient n were determined by plotting the fractional activity as a function of amine concentration c and fitting them to the Hill equation

$$Y = Y_0 + (Y_{MAX} - Y_0)/\{1 + (EC_{50}/c)^n\}$$

where Y_0 is Y without polypeptide, Y_{MAX} is Y with 1.0% triton X-100 instead of polypeptides, i.e., 100% CF efflux, EC_{50} is the concentration of polypeptide required to reach 50% activity, and n is the Hill coefficient.

RESULTS AND DISCUSSION

To generate ionic polypeptides with various EG_x linkers, we prepared three L-glutamate-based monomers denoted as EG_xene-GluNCA (x = 1−3). All monomers were synthesized in a concise and straightforward manner within 3 steps. Briefly, bishydroxy-terminated oligo(ethylene glycol) (HO-EG_x-OH) were reacted with 3-bromopropene to etherize one hydroxyl group to generate HO-EG_xene, which were then esterified by reacting with L-glutamic acid to afford EG_x-ylated L-glutamate derivatives EG_xene-Glu. The EG_xene-Glu were converted to the corresponding EG_xene-GluNCA in dry THF using triphosgene and purified by column chromatography in ambient atmosphere with ∼60−80% yield. All precursors and monomers were comprehensively characterized (Figures S1−S16). Next, we polymerized EG_xene-GluNCA by using hexamethyldisilazane (HMDS) as the initiator (Scheme 1). At the feeding monomer/initiator ratio (M:I) of 20:1, 50:1, and 100:1, gel permeation chromatography (GPC) gave monomodal peaks for all resultant P(EG_xene-Glu) polymers with controlled molecular weights (MW) and low polydispersity indices ($Đ$) (Table 1 and Figure S17). ^{1}H NMR spectra of P(EG_xene-Glu) exhibited characteristic allyl peaks (Figures S18−S20). Next, we functionalized P(EG_xene-Glu)$_{50}$ via the thiol−ene chemistry by using *N,N*-dimethyl mercaptoethylamine hydrochloride to afford the highly water-soluble P(EG_xDMA-Glu)$_{50}$. The tertiary amine was selected here because Gao et al. have previously demonstrated that tertiary amines have tunable apparent pK_a near the physiological range.[40] The alkene peaks disappeared completely in the ^{1}H NMR spectra of the purified P(EG_xDMA-Glu)$_{50}$, which suggested a nearly 100% grafting efficiency (Figures S21−S23).

Table 1. HMDS-Mediated ROP of EG_xene-GluNCAs[a]

entry	monomer	$DP_{exp.}$[b]	$DP_{obt.}$[c]	$M_{Wobt.}$ (g mol^{-1})[d]	$Đ$[e]
1	EG_1ene-GluNCA	50	52	11200	1.12
2	EG_2ene-GluNCA	50	54	14000	1.13
3	EG_3ene-GluNCA	20	25	7700	1.04
4	EG_3ene-GluNCA	50	55	16720	1.09
5	EG_3ene-GluNCA	100	105	31900	1.05

[a]All polymerizations were analyzed at more than 95% monomer conversion, which was determined by monitoring the NCA anhydride peak at 1853 cm^{-1} in FT-IR spectroscopy. [b]$DP_{exp.}$ = expected degree of polymerization (feeding M/I ratio). [c]$DP_{obt.}$ = obtained degree of polymerization, the dn/dc values of P(EG_xene-Glu) were determined to be 0.0465 (x = 1), 0.0547 (x = 2), and 0.0590 (x = 3) mL/g. [d]$M_{Wobt.}$ = molecular weight obtained. [e]$Đ$ = polydispersity index, determined by GPC.

For the pH-induced helix−coil transition of P(EG_xDMA-Glu)$_{50}$ to be studied, all of the samples were dissolved in ultrapure water at 0.05 mg/mL. The pH values of all solutions were carefully adjusted by either 1 M HCl or NaOH and measured by a pH meter. CD spectra of the polymers depicted a rapid and characteristic coil-to-helix transition as the pH increased from ∼3 to 9 (Figure 1A and Figure S24). The maximum helicities of the polymers were measured to be ∼80−84%, which were fairly high for 50-mer polypeptides. Next, the helicity was plotted as a function of pH to compare the pH-induced coil-to-helix transition of all polymers (Figure 1B). For clarity and simplicity purposes, we defined the pH as the halfway transition point (H_{50}-pH) when a polymer adopts 50% of its maximum helicity. Interestingly, the H_{50}-pH of P(EG_xDMA-Glu)$_{50}$ was measured as ∼5.3 (x = 1), 5.5 (x = 2), and 6.8 (x = 3). In contrast, the H_{50}-pH of PLL was ∼10.6. Titration of P(EG_xDMA-Glu)$_{50}$ and PLL by NaOH (Figure S25) implied that the apparent pK_a values (defined as the pH when 50% of all the ionizable amines are protonated) of the polymers correlated with their H_{50}-pHs fairly well (Table S1).[40] Thus, it appeared that the coil-to-helix transition of P(EG_xDMA-Glu)$_{50}$ was dependent on the protonation status of the tertiary amines, similar to PLL.

We then examined the salt effect by gradually increasing the salt concentration in P(EG_xDMA-Glu)$_{50}$ solutions. As shown in Figure 2A and Figure S26, all P(EG_xDMA-Glu)$_{50}$ exhibited an unexpected but clear salt-induced coil-to-helix transition when the polymers were initially in the unfolded state at an acidic pH (e.g., 4.5). Maximum helicities were reached with the addition of ∼120 mM NaCl. In sharp contrast, PLL did not show any sign of helical conformation even at 500 mM NaCl, the highest salt concentration we tested. When all polymers initially adopted high helical contents (e.g., at basic pHs), P(EG_xDMA-Glu)$_{50}$ were found to have slightly enhanced helicity following the addition of NaCl, whereas PLL showed a helix-to-coil conformational switch under the same conditions (Figure 2B and Figure S26). Thus, it was clear that P(EG_xDMA-Glu)$_{50}$ and PLL had completely opposite conformational switches with respect to salt. To examine the conformational transition in different lyotropic salts, we also measured the CD spectra of

DOI: 10.1021/acs.biomac.8b00204
Biomacromolecules 2018, 19, 2089−2097

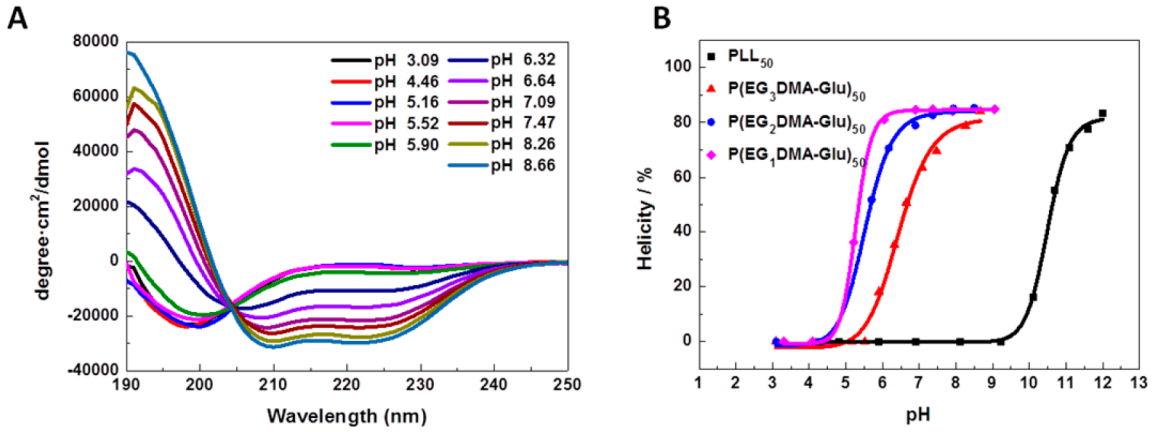

Figure 1. pH-dependent coil-to-helix transition. (A) Overlay of CD spectra of $P(EG_3DMA\text{-}Glu)_{50}$ at various pHs. (B) pH-dependent helicity of $P(EG_xDMA\text{-}Glu)_{50}$ and PLL_{50}. The helicity was calculated using the following equation: helicity = $(-[\theta_{222}] + 3000)/39000 \times 100\%$.[42]

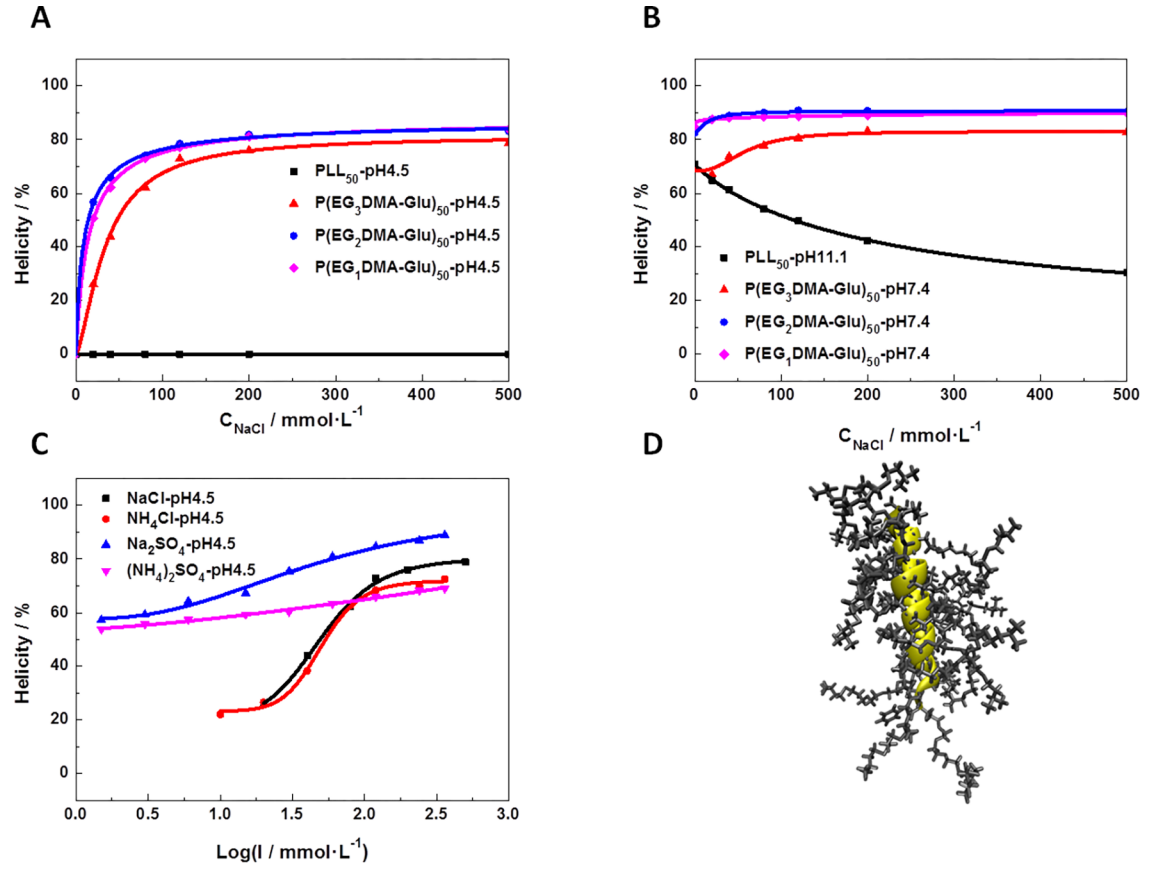

Figure 2. Salt-induced helix formation. (A,B) The helicity of $P(EG_xDMA\text{-}Glu)_{50}$ and PLL_{50} as a function of NaCl concentration (A) when all polymers initially adopted a coiled conformation (pH 4.5) (B) under conditions when all polymers initially adopted a helical conformation (pH 7.4 for $P(EG_xDMA\text{-}Glu)_{50}$ and 11.1 for PLL_{50}). (C) The helicity of $P(EG_3DMA\text{-}Glu)_{50}$ as a function of the logarithm of ionic strength in four different salts: NaCl, NH_4Cl, Na_2SO_4, and $(NH_4)_2SO_4$. (D) MD simulation of $P(EG_3DMA\text{-}Glu)_{20}$ in NaCl solution with fully charged side chains (50 ns).

$P(EG_3DMA\text{-}Glu)_{50}$ in $(NH_4)_2SO_4$, Na_2SO_4, and NH_4Cl at pH 4.5. To facilitate the direct comparison between different salts, the helicity of the polymer was plotted as a function of the logarithm of ionic strength (log I). Upon the increase in ionic strength, interestingly, $P(EG_3DMA\text{-}Glu)_{50}$ adopted a more sensitive coil-to-helix transition in the kosmotropic $(NH_4)_2SO_4$ and Na_2SO_4 than in NaCl and NH_4Cl (Figure 2C and Figure S27). Moreover, it appeared that the anion had a greater salting-out effect than that of the cation, which was also observed in proteins.[43] Overall, the results indicated that the synthetic polypeptides followed a similar trend with proteins as far as the interaction with different Hofmeister salts was concerned. To verify the stable α-helix of the ionic polypeptides at low pH with salt, we performed all-atom MD simulation, a method that has been widely used for protein conformation analysis.[44] $P(EG_3DMA\text{-}Glu)_{20}$ was selected as a model polypeptide and simulated using the AMBER12 suite of programs. All of the terminal amine groups were protonated to simulate the low pH environment. During the 50 ns simulation, the fully charged $P(EG_3DMA\text{-}Glu)_{20}$ remained in

DOI: 10.1021/acs.biomac.8b00204
Biomacromolecules 2018, 19, 2089−2097

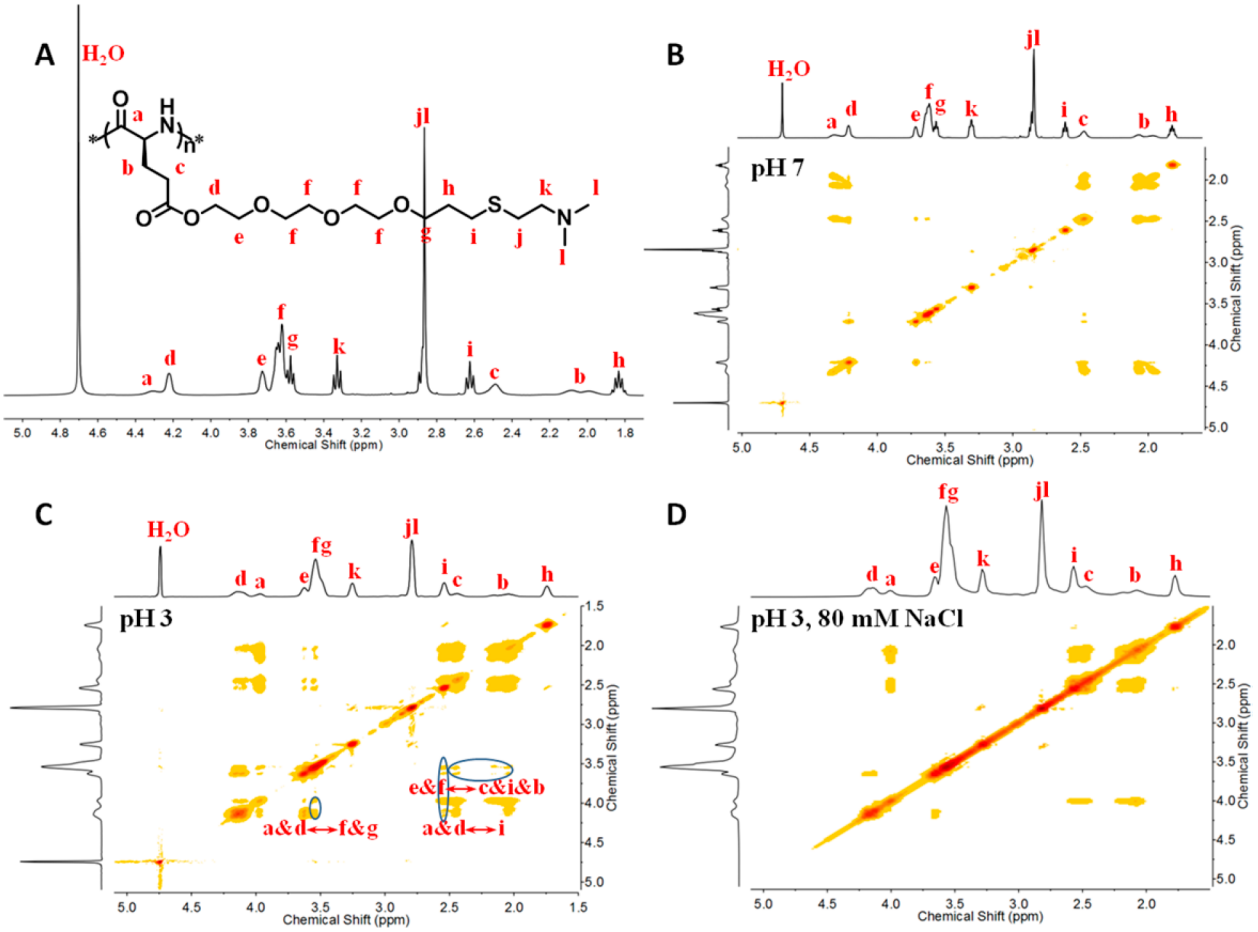

Figure 3. (A) ^{1}H NMR spectra of P(EG$_3$DMA-Glu)$_{50}$. (B–D) 2D NOESY spectra of P(EG$_3$DMA-Glu)$_{50}$ at pH 7 and no salt (B), at pH 3 and no salt (C), and at pH 3 with 80 mM NaCl (D). The blue circles represent additional NOE signals when P(EG$_3$DMA-Glu)$_{50}$ is in coiled conformation.

an intact α-helix conformation in NaCl solution, highlighting the robustness of our ionic helical polypeptides (Figure 2D and Supporting Movie). Moreover, the helicities of P(EG$_x$DMA-Glu)$_{50}$ decreased only slightly even at a temperature up to 70 °C, further underscoring their excellent helical thermostability (Figure S28).

Next, we conducted 2D NOESY experiments to investigate the chemical environment of P(EG$_x$DMA-Glu)$_{50}$ at different pH and ionic strengths (Figure 3).[45] Taking P(EG$_3$DMA-Glu)$_{50}$ in D_2O as an example, no cross peaks belonging to NOE signals were observed in the spectrum at pH 7 (Figure 3B). Interestingly, when the solution was acidified to pH 3, several cross peaks attributable to the NOE signals were clearly seen (Figure 3C). For example, the spectrum suggested that the EG$_3$ linker protons (H$_e$ and H$_f$) and the glutamate protons (H$_b$ and H$_c$) were spatially in close contact with each other (<0.5 nm) as evidenced by the NOE cross peaks. The protons of the inner methylene adjacent to the thioether (H$_i$) also showed considerable crosstalk with protons structurally far away from them (e.g., H$_a$, H$_d$, H$_e$, and H$_f$). Together, the spectra implied the occurrence of intramolecular entanglement of side chains when the backbone of P(EG$_x$DMA-Glu)$_{50}$ underwent a helix-to-coil transition from pH 7 to 3. Moreover, when the polymer restored its helicity at pH 3 by the aid of 80 mM NaCl, the NOESY spectrum once again gave no obvious NOE peaks and appeared very similar to the spectrum at pH 7 without salt (Figure 3B and D). It was worth mentioning that no signal was detected for all solutions in dynamic light scattering (DLS), suggesting there was no aggregation under the conditions tested and thus ruling out the possibility of intermolecular interaction-induced NOE effect (data not shown). Similar NOESY results were obtained for both P(EG$_1$DMA-Glu)$_{50}$ and P(EG$_2$DMA-Glu)$_{50}$ (Figures S29 and S30).

On the basis of the experimental results and the simulation, we proposed our prototype model for the pH- and salt-induced coil-to-helix transition of P(EG$_x$DMA-Glu) (Figure 4). At a relatively basic pH in water (e.g., >7.0), it was not surprising that the neutral polymers all adopted the α-helical conformation. Notably, P(EG$_x$DMA-Glu) were highly soluble in water because of the hydrophilic EG$_x$ linkers and the terminal amines, even at the electronic neutral form. When the tertiary amines were protonated at an acidic pH, the charge repulsion became predominate and led to the disruption of the helix, similar to PLL. Nevertheless, the transition pH shifted to 5.5–6.5 due to the presence of the EG$_x$ and the thioether linkers. With the addition of salt, the helix was restored owing to two possible reasons. One potential reason was the screen effect of the salt that could shield the side chain charge repulsion. Although this screen effect was also applicable to PLL, one should be aware that the charge repulsion in PLL was appreciably greater than that in P(EG$_x$DMA-Glu) because the CBD of PLL (5 σ bonds) was significantly shorter relative to P(EG$_x$DMA-Glu) (14, 22, and 30 σ bonds for EG$_1$, EG$_2$, and EG$_3$, respectively). Another reason was attributable to the amphiphilicity of the EG$_x$ linker. It was postulated that the salt in solution could compete for water molecules with the EG$_x$

DOI: 10.1021/acs.biomac.8b00204
Biomacromolecules 2018, 19, 2089–2097

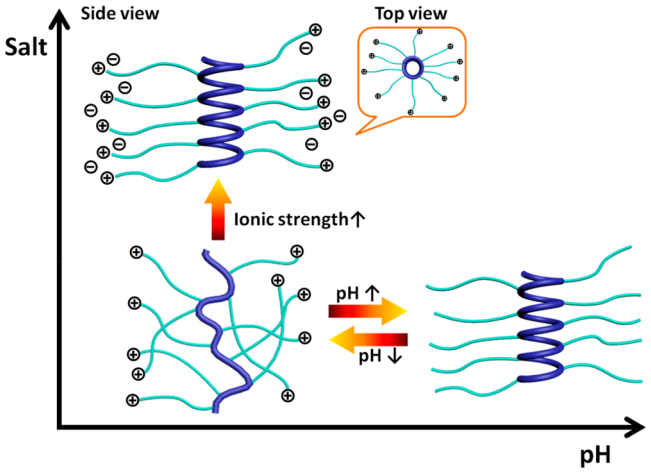

Figure 4. Cartoon illustration of the pH- and salt-induced conformation transition of P(EG_xDMA-Glu).

linker, which altered the hydration state of the inner side chain and ultimately led to enhanced helicity of the polypeptides.[37,46] With more rigorous works underway with our collaborators, we expect to report the more detailed biophysical mechanism and theoretical prediction in a separate work later.

Ionic helical polypeptides are promising biomaterials for their helicity-induced transmembrane activity.[47−49] However, the linker chemistry has not yet been fully explored to achieve balanced toxicity and activity. To this end, we evaluated the toxicity and the membrane activity of P(EG_xDMA-Glu)$_{50}$. MTT assay results using 4T1 cells indicated that the IC_{50} of P(EG_xDMA-Glu)$_{50}$ was 96.9 (x = 1), 264.5 (x = 2), and >500 (x = 3) μg/mL, respectively (Figure 5A and Table S2). We also studied the membrane activity of the polymers by using LUVs⊃CF, i.e., large unilamellar vesicles (LUVs) composed of the 1, 2-dioleoyl-*sn*-glycero-3-phosphocholine (DOPC), cholesterol, and distearoyl phosphoethanolamine-PEG2000 (DSPE-PEG2000) and loaded with 5(6)-carboxyfluorescein (CF) (Figure 5B and Table S2).[41] Interestingly, the membrane disruption EC_{50} of P(EG_3DMA-Glu)$_{50}$ was measured to be 0.0108 μg/mL, ∼6−10-fold more potent than P(EG_2DMA-Glu)$_{50}$ (EC_{50} ≈ 0.123 μg/mL) and P(EG_1DMA-Glu)$_{50}$ (EC_{50} ≈ 0.0657 μg/mL). Together, the data suggested that, by elongating the repeating unit of the EG linker, the polymer could gain higher membrane activity with lower cytotoxicity.

CONCLUSIONS

In conclusion, we successfully synthesized a series of tertiary amine-functionalized EG_x-linked polypeptide electrolytes. The resultant P(EG_xDMA-Glu) polymers showed excellent aqueous solubility regardless of their charge states. Unlike PLL that can form a helix only at a pH above 10, CD spectroscopy indicated that P(EG_xDMA-Glu) underwent a pH-dependent coil-to-helix switch right within the physiological range. More interestingly, P(EG_xDMA-Glu) exhibited unusual salt-induced helical conformation owing to the unique properties of EG_x linkers. Preliminary studies indicated that P(EG_3DMA-Glu) was considerably less toxic but in the meantime preserved an appreciable higher membrane activity compared to its analogues P(EG_1DMA-Glu) and P(EG_2DMA-Glu). The current work thus highlights the importance of fine-tuning the linker chemistry in achieving conformation-switchable polypeptides and represents a facile approach toward stimuli-responsive biopolymers for advanced biological applications.

ASSOCIATED CONTENT

Supporting Information

The Supporting Information is available free of charge on the ACS Publications website at DOI: 10.1021/acs.biomac.8b00204.

Characterization data (^{1}H NMR, ^{13}C NMR, MS), GPC curves, CD spectra, pH titration curves, and NOESY spectra (PDF)

A supporting movie (MPG)

AUTHOR INFORMATION

Corresponding Authors

*E-mail: chemhualu@pku.edu.cn.

*E-mail: lijiangy@pku.edu.cn.

ORCID

Hua Lu: 0000-0003-2180-3091

Notes

The authors declare no competing financial interest.

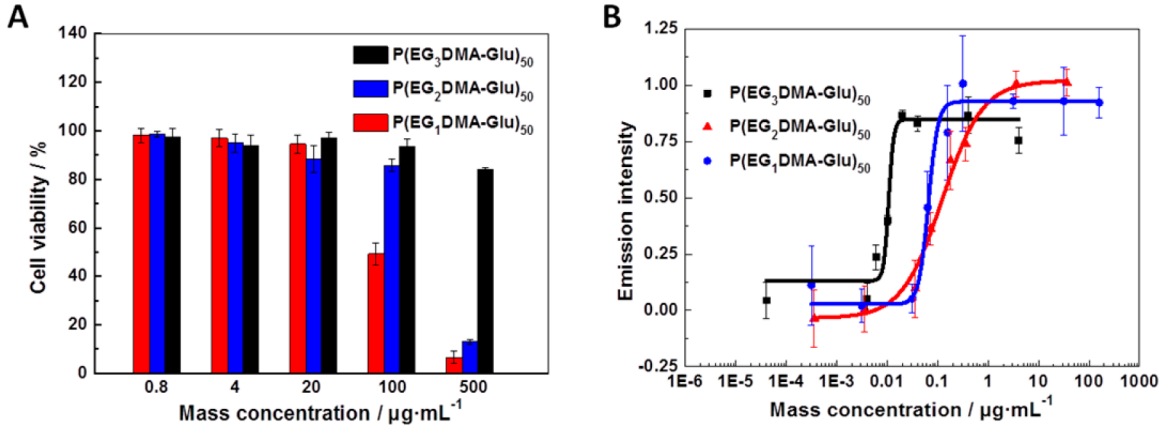

Figure 5. (A) Cytotoxicity of P(EG_xDMA-Glu)$_{50}$ toward 4T1 cancer cells measured by the MTT assay. (B) Membrane activity of P(EG_xDMA-Glu)$_{50}$ assessed using CF-loaded LUVs.

DOI: 10.1021/acs.biomac.8b00204
Biomacromolecules 2018, 19, 2089−2097

■ ACKNOWLEDGMENTS

This work is supported by the National Natural Science Foundation of China (21722401, 21474004, 21434008, and U1430237). H.L. thanks the support from the Youth Thousand-Talents Program of China. We gratefully acknowledge Dr. Yuting Sun and Prof. Xing Chen for the help in membrane activity experiments and Hailin Fu and Prof. Yao Lin for the discussion of the physical model.

■ REFERENCES

(1) Schmidt, N. W.; Wong, G. C. Antimicrobial peptides and induced membrane curvature: geometry, coordination chemistry, and molecular engineering. *Curr. Opin. Solid State Mater. Sci.* **2013**, *17*, 151−163.
(2) Bryson, J. W.; Betz, S. F.; Lu, H. S.; Suich, D. J.; Zhou, H. X.; O'Neil, K. T.; DeGrado, W. F. Protein design: a hierarchic approach. *Science* **1995**, *270*, 935−941.
(3) Derossi, D.; Calvet, S.; Trembleau, A.; Brunissen, A.; Chassaing, G.; Prochiantz, A. Cell internalization of the third helix of the Antennapedia homeodomain is receptor-independent. *J. Biol. Chem.* **1996**, *271*, 18188−19193.
(4) Oren, Z.; Ramesh, J.; Avrahami, D.; Suryaprakash, N.; Shai, Y.; Jelinek, R. Structures and mode of membrane interaction of a short alpha helical lytic peptide and its diastereomer determined by NMR, FTIR, and fluorescence spectroscopy. *Eur. J. Biochem.* **2002**, *269*, 3869−3880.
(5) Oren, Z.; Shai, Y. Cyclization of a cytolytic amphipathic alpha-helical peptide and its diastereomer: effect on structure, interaction with model membranes, and biological function. *Biochemistry* **2000**, *39*, 6103−6114.
(6) Goodman, C. M.; Choi, S.; Shandler, S.; DeGrado, W. F. Foldamers as versatile frameworks for the design and evolution of function. *Nat. Chem. Biol.* **2007**, *3*, 252−262.
(7) Gabriel, G. J.; Tew, G. N. Conformationally rigid proteomimetics: a case study in designing antimicrobial aryl oligomers. *Org. Biomol. Chem.* **2008**, *6*, 417−423.
(8) Hite, K. C.; Kalashnikova, A. A.; Hansen, J. C. Coil-to-helix transitions in intrinsically disordered methyl CpG binding protein 2 and its isolated domains. *Protein Sci.* **2012**, *21*, 531−538.
(9) Karanth, N. M.; Sarma, S. P. The coil-to-helix transition in ilvn regulates the allosteric control of escherichia coli acetohydroxyacid synthase I. *Biochemistry* **2013**, *52*, 70−83.
(10) Xiong, M.; Han, Z.; Song, Z.; Yu, J.; Ying, H.; Yin, L.; Cheng, J. Bacteria-assisted activation of antimicrobial polypeptides by a random-coil to helix transition. *Angew. Chem., Int. Ed.* **2017**, *56*, 10826−10829.
(11) Wyatt, L. C.; Lewis, J. S.; Andreev, O. A.; Reshetnyak, Y. K.; Engelman, D. M. Applications of phlip technology for cancer imaging and therapy. *Trends Biotechnol.* **2017**, *35*, 653−664.
(12) Tapmeier, T. T.; Moshnikova, A.; Beech, J.; Allen, D.; Kinchesh, P.; Smart, S.; Harris, A.; McIntyre, A.; Engelman, D. M.; Andreev, O. A.; Reshetnyak, Y. K.; Muschel, R. J. The pH low insertion peptide pHLIP Variant 3 as a novel marker of acidic malignant lesions. *Proc. Natl. Acad. Sci. U. S. A.* **2015**, *112*, 9710−9715.
(13) Andreev, O. A.; Karabadzhak, A. G.; Weerakkody, D.; Andreev, G. O.; Engelman, D. M.; Reshetnyak, Y. K. pH (low) insertion peptide (pHLIP) inserts across a lipid bilayer as a helix and exits by a different path. *Proc. Natl. Acad. Sci. U. S. A.* **2010**, *107*, 4081−4086.
(14) Huang, J.; Heise, A. Stimuli responsive synthetic polypeptides derived from *N*-carboxyanhydride (NCA) polymerisation. *Chem. Soc. Rev.* **2013**, *42*, 7373−7390.
(15) Shen, Y.; Fu, X.; Fu, W.; Li, Z. Biodegradable stimuli-responsive polypeptide materials prepared by ring opening polymerization. *Chem. Soc. Rev.* **2015**, *44*, 612−622.
(16) Bonduelle, C. Secondary structures of synthetic polypeptide polymers. *Polym. Chem.* **2018**, *9*, 1517.
(17) Deming, T. J. Facile synthesis of block copolypeptides of defined architecture. *Nature* **1997**, *390*, 386−389.
(18) Zhao, W.; Gnanou, Y.; Hadjichristidis, N. Fast and living ring-opening polymerization of α-amino acid *N*-carboxyanhydrides triggered by an "alliance" of primary and secondary amines at room temperature. *Biomacromolecules* **2015**, *16*, 1352−1357.
(19) Zou, J.; Fan, J.; He, X.; Zhang, S.; Wang, H.; Wooley, K. L. A facile glovebox-free strategy to significantly accelerate the syntheses of well-defined polypeptides by *N*-carboxyanhydride (NCA) ring-opening polymerizations. *Macromolecules* **2013**, *46*, 4223−4226.
(20) Conejos-Sanchez, I.; Duro-Castano, A.; Birke, A.; Barz, M.; Vicent, M. J. A controlled and versatile NCA polymerization method for the synthesis of polypeptides. *Polym. Chem.* **2013**, *4*, 3182−3186.
(21) Peng, H.; Ling, J.; Zhu, Y.; You, L.; Shen, Z. Polymerization of α-amino acid *N*-carboxyanhydrides catalyzed by rare earth tris(borohydride) complexes: mechanism and hydroxy-endcapped polypeptides. *J. Polym. Sci., Part A: Polym. Chem.* **2012**, *50*, 3016−3029.
(22) Habraken, G. J. M.; Wilsens, K. H. R. M.; Koning, C. E.; Heise, A. Optimization of *N*-carboxyanhydride (NCA) polymerization by variation of reaction temperature and pressure. *Polym. Chem.* **2011**, *2*, 1322−1330.
(23) Li, P.; Dong, C. M. Phototriggered ring-opening polymerization of a photocaged L-lysine *N*-carboxyanhydride to synthesize hyperbranched and linear polypeptides. *ACS Macro Lett.* **2017**, *6*, 292−297.
(24) Wu, X. J.; Zhou, L. Z.; Su, Y.; Dong, C. M. Comb-like poly(L-cysteine) derivatives with different side groups: synthesis via photochemistry and click chemistry, multi-responsive nanostructures, triggered drug release and cytotoxicity. *Polym. Chem.* **2015**, *6*, 6857−6869.
(25) Zhang, Y.; Lu, H.; Lin, Y.; Cheng, J. Water-soluble polypeptides with elongated, charged side chains adopt ultra-stable helical conformations. *Macromolecules* **2011**, *44*, 6641−6644.
(26) Lu, H.; Wang, J.; Bai, Y. G.; Lang, J. W.; Liu, S. Y.; Lin, Y.; Cheng, J. J. Ionic polypeptides with unusual helical stability. *Nat. Commun.* **2011**, *2*, 206.
(27) Kramer, J. R.; Deming, T. J. Glycopolypeptides with a redox-triggered helix-to-coil transition. *J. Am. Chem. Soc.* **2012**, *134*, 4112−4115.
(28) Fu, X. H.; Ma, Y. A.; Shen, Y.; Fu, W. X.; Li, Z. B. Oxidation-responsive OEGylated poly-L-cysteine and solution properties studies. *Biomacromolecules* **2014**, *15*, 1055−1061.
(29) Xiong, W.; Fu, X. H.; Wan, Y. M.; Sun, Y. L.; Li, Z. B.; Lu, H. Synthesis and multimodal responsiveness of poly(alpha-amino acid)s bearing OEGylated azobenzene side-chains. *Polym. Chem.* **2016**, *7*, 6375−6382.
(30) Bonduelle, C.; Makni, F.; Severac, L.; Piedra-Arroni, E.; Serpentini, C.-L.; Lecommandoux, S.; Pratviel, G. Smart metallopoly(L-glutamic acid) polymers: reversible helix-to-coil transition at neutral pH. *RSC Adv.* **2016**, *6*, 84694−84697.
(31) Krannig, K. S.; Schlaad, H. pH-responsive bioactive glycopolypeptides with enhanced helicity and solubility in aqueous solution. *J. Am. Chem. Soc.* **2012**, *134*, 18542−18545.
(32) Krannig, K. S.; Sun, J.; Schlaad, H. Stimuli-responsivity of secondary structures of glycopolypeptides derived from poly(L-glutamate-co-allylglycine). *Biomacromolecules* **2014**, *15*, 978−984.
(33) Piedra-Arroni, E.; Makni, F.; Severac, L.; Stigliani, J.-L.; Pratviel, G.; Bonduelle, C. Smart Poly(imidazoyl-l-lysine): Synthesis and reversible helix-to-coil transition at neutral pH. *Polymers* **2017**, *9*, 276.
(34) Song, Z.; Mansbach, R. A.; He, H.; Shih, K. C.; Baumgartner, R.; Zheng, N.; Ba, X.; Huang, Y.; Mani, D.; Liu, Y.; Lin, Y.; Nieh, M. P.; Ferguson, A. L.; Yin, L.; Cheng, J. Modulation of polypeptide conformation through donor-acceptor transformation of side-chain hydrogen bonding ligands. *Nat. Commun.* **2017**, *8*, 92.
(35) Silverio, S. C.; Rodriguez, O.; Teixeira, J. A.; Macedo, E. A. The effect of salts on the liquid-liquid phase equilibria of PEG600+salt aqueous two-phase systems. *J. Chem. Eng. Data* **2013**, *58*, 3528−3535.
(36) Tao, X. F.; Deng, C.; Ling, J. PEG-amine-initiated polymerization of sarcosine *N*-thiocarboxyanhydrides toward novel double-hydrophilic PEG-*b*-polysarcosine diblock copolymers. *Macromol. Rapid Commun.* **2014**, *35*, 875−881.
(37) Ke, F. Y.; Mo, X. L.; Yang, R. M.; Wang, Y. M.; Liang, D. H. Association of block copolymer in nonselective solvent. *Macromolecules* **2009**, *42*, 5339−5344.

DOI: 10.1021/acs.biomac.8b00204
Biomacromolecules 2018, 19, 2089−2097

(38) Casse, O.; Shkilnyy, A.; Linders, J.; Mayer, C.; Haussinger, D.; Volkel, A.; Thunemann, A. F.; Dimova, R.; Colfen, H.; Meier, W.; Schlaad, H.; Taubert, A. Solution behavior of double-hydrophilic block copolymers in dilute aqueous solution. *Macromolecules* **2012**, *45*, 4772−4777.
(39) Yuan, J.; Sun, Y.; Wang, J.; Lu, H. Phenyl trimethylsilyl sulfide-mediated controlled ring-opening polymerization of α-amino acid *N*-carboxyanhydrides. *Biomacromolecules* **2016**, *17*, 891−896.
(40) Li, Y.; Zhao, T.; Wang, C.; Lin, Z.; Huang, G.; Sumer, B. D.; Gao, J. Molecular basis of cooperativity in pH-triggered supramolecular self-assembly. *Nat. Commun.* **2016**, *7*, 13214.
(41) Bang, E. K.; Gasparini, G.; Molinard, G.; Roux, A.; Sakai, N.; Matile, S. Substrate-initiated synthesis of cell-penetrating poly(disulfide)s. *J. Am. Chem. Soc.* **2013**, *135*, 2088−2091.
(42) Chen, C.; Wang, Z.; Li, Z. Thermoresponsive polypeptides from pegylated poly-L-glutamates. *Biomacromolecules* **2011**, *12*, 2859−2863.
(43) Zhang, Y.; Cremer, P. Interactions between macromolecules and ions: the Hofmeister series. *Curr. Opin. Chem. Biol.* **2006**, *10*, 658−663.
(44) Karplus, M.; McCammon, J. A. Molecular dynamics simulations of biomolecules. *Nat. Struct. Biol.* **2002**, *9*, 646−652.
(45) Ren, Y.; Baumgartner, R.; Fu, H.; van der Schoot, P.; Cheng, J.; Lin, Y. Revisiting the helical cooperativity of synthetic polypeptides in solution. *Biomacromolecules* **2017**, *18*, 2324−2332.
(46) Keefe, A. J.; Jiang, S. Y. Poly(zwitterionic)protein conjugates offer increased stability without sacrificing binding affinity or bioactivity. *Nat. Chem.* **2012**, *4*, 60−64.
(47) Xiong, M.; Lee, M. W.; Mansbach, R. A.; Song, Z.; Bao, Y.; Peek, R. M., Jr.; Yao, C.; Chen, L. F.; Ferguson, A. L.; Wong, G. C.; Cheng, J. Helical antimicrobial polypeptides with radial amphiphilicity. *Proc. Natl. Acad. Sci. U. S. A.* **2015**, *112*, 13155−13160.
(48) Zhang, R.; Song, Z.; Yin, L.; Zheng, N.; Tang, H.; Lu, H.; Gabrielson, N. P.; Lin, Y.; Kim, K.; Cheng, J. Ionic α-helical polypeptides toward nonviral gene delivery. *WIRES Nanomed. Nanobi.* **2015**, *7*, 98−110.
(49) Brogden, K. A. Antimicrobial peptides: pore formers or metabolic inhibitors in bacteria? *Nat. Rev. Microbiol.* **2005**, *3*, 238−250.

DOI: 10.1021/acs.biomac.8b00204
Biomacromolecules 2018, 19, 2089−2097